# Is the chemical gate of connexins voltage sensitive? Behavior of Cx32 wild-type and mutant channels

CAMILLO PERACCHIA, XIAO G. WANG, AND LILLIAN L. PERACCHIA
*Department of Pharmacology and Physiology, School of Medicine and Dentistry, University of Rochester, Rochester, New York 14642-8711*

**Peracchia, Camillo, Xiao G. Wang, and Lillian L. Peracchia.** Is the chemical gate of connexins voltage sensitive? Behavior of Cx32 wild-type and mutant channels. *Am. J. Physiol.* 276 (*Cell Physiol.* 45): C1361–C1373, 1999.—Connexin channels are gated by transjunctional voltage ($V_j$) or $CO_2$ via distinct mechanisms. The cytoplasmic loop (CL) and arginines of a COOH-terminal domain ($CT_1$) of connexin32 (Cx32) were shown to determine $CO_2$ sensitivity, and a gating mechanism involving CL-$CT_1$ association-dissociation was proposed. This study reports that Cx32 mutants, tandem, 5R/E, and 5R/N, designed to weaken CL-$CT_1$ interactions, display atypical $V_j$ and $CO_2$ sensitivities when tested heterotypically with Cx32 wild-type channels in *Xenopus* oocytes. In tandems, two Cx32 monomers are linked $NH_2$-to-COOH terminus. In 5R/E and 5R/N mutants, glutamates or asparagines replace $CT_1$ arginines. On the basis of the intriguing sensitivity of the mutant-32 channel to $V_j$ polarity, the existence of a "slow gate" distinct from the conventional $V_j$ gate is proposed. To a lesser extent the slow gate manifests itself also in homotypic Cx32 channels. Mutant-32 channels are more $CO_2$ sensitive than homotypic Cx32 channels, and $CO_2$-induced chemical gating is reversed with relative depolarization of the mutant oocyte, suggesting $V_j$ sensitivity of chemical gating. A hypothetical pore-plugging model involving an acidic cytosolic protein (possibly calmodulin) is discussed.

cell communication; cell junctions; pH gating

GAP JUNCTIONS ARE MEMBRANE differentiations specialized for direct cell-to-cell exchange of metabolic and electrical signals. A gap junction channel is made of two hemichannels (connexons), each a hexamer of connexin proteins. Connexins have four transmembrane domains linked by two extracellular loops and a cytoplasmic loop (CL), a short $NH_2$ terminus (NT), and a COOH terminus (CT) of variable length (for review see Ref. 13).

Gap junction channels close in response to changes in transjunctional voltage ($V_j$) or intracellular $Ca^{2+}$ or $H^+$ concentration (for review see Refs. 3, 9, and 14), but the molecular mechanisms of channel gating are still unclear. $V_j$ and chemical gates are believed to be two distinct gates: the former closes the channel rapidly but incompletely, and the latter closes the channel slowly but completely (5).

Recently, we studied connexin mutants and chimeras expressed in *Xenopus* oocytes to identify domains of the rat connexin32 (Cx32) potentially involved in $CO_2$-induced (low intracellular pH) channel gating. Cx32 is a connexin expressed in many organs, such as liver, pancreas, kidney, thyroid, and mammary gland, and in various cells of the nervous system, such as neurons, oligodendrocytes, and Schwann cells (for review see Ref. 3). Several Cx32 mutations have been shown to be relevant to the pathogenesis of a demyelinating disease known as the X-linked Charcot-Marie-Tooth disease (2, 3).

In Cx32, CL contains a domain relevant to $CO_2$ gating sensitivity (23, 24), and NT (23) and 84% of CT (25, 28, 30) do not seem to play a role, whereas basic residues of the initial domain of CT ($CT_1$) inhibit $CO_2$ gating sensitivity (25, 28). Thus Cx32 appears to differ from Cx43, in which CT seems to play a major role in chemical gating (8) via a postulated ball-and-chain mechanism (6, 10). On the basis of our work on Cx32, we have proposed that $CT_1$, a basic and partly hydrophobic domain, may interact electrostatically and hydrophobically with acidic and hydrophobic residues of $CL_1$ and may inhibit gating by latching CL (26).

To further probe the chemical gating mechanism of Cx32, three new mutants were constructed. One mutant, the tandem, is a dimer in which two Cx32 monomers are concatenated NT-to-CT. With this mutant, each connexon (hemichannel) is made of three tandem connexins. In each connexon, three of the six NT chains are linked to three CT chains and the other three NT and CT chains are free. Another mutant, the 5R/E, is a Cx32 molecule in which five basic residues of $CT_1$ (R215, R219, R220, R223, and R224) are replaced with an acidic residue (E). In the third mutant, the 5R/N, the five basic $CT_1$ residues mentioned above are replaced with a neutral-polar residue (N). This mutant, when tested homotypically, generated channels more sensitive to $CO_2$ than Cx32 (25, 28). All these mutations would be expected to interfere with the $CT_1$-$CL_1$ interaction. Homotypic pairing of tandem and 5R/E mutants did not produce functional junctions.

The data show that, in all these heterotypic channels, junctional conductance ($G_j$) increases with $V_j$ gradients positive at the tandem, 5R/E, or 5R/N side and decreases with $V_j$ of opposite polarity. In addition, positive $V_j$ gradients partially reverse the $G_j$ drop induced by $CO_2$, suggesting that the chemical gate might be voltage sensitive.

## MATERIALS AND METHODS

### *Site-Directed Mutagenesis*

Molecular biology protocols were generally as described by Sambrook et al. (20). Cx32 cDNA (12) was used in the construction of DNA mutants. Two wild-type Cx32 were

The costs of publication of this article were defrayed in part by the payment of page charges. The article must therefore be hereby marked "*advertisement*" in accordance with 18 U.S.C. Section 1734 solely to indicate this fact.

linked to form a Cx32 tandem; a tandem is a Cx32 dimer composed of two Cx32 monomers concatenated NT-to-CT. Normal and modified Cx32 cDNAs were used in the construction of the tandem. The modification involved the deletion of a silent stop codon preceding the ATG initiation codon, which would be used in the second Cx32 monomer of the tandem. The strategy employed to create the 5R/E and 5R/N mutants of Cx32 has been previously described (25). All the mutations were verified by digestion of DNA with restriction enzymes and sequence analysis.

### *Oligonucleotide Sequences*

Oligonucleotides were synthesized by a DNA synthesizer (model 393, ABI, Foster City, CA). The sequences used to produce the 5R/E and 5R/N mutants are as follows (underscored letters represent mutated nucleotides): 5′-CCTT GCGGGAGGGCGGATTAGATTCCTCCTGAGCTTCCTC (5R/E) and 5′-CCTTGCGGGAGGGCGGATTGGAGTTGTTCTGAGC GTTGTT (5R/N).

### *Preparation of cRNA*

Wild-type and mutated forms of Cx32 cDNA were subcloned into pBluescript (Stratagene, Menasha, WI) or pGEM 3Z (Promega, Madison, WI) and used for in vitro synthesis of cRNA. cRNAs were transcribed from linearized plasmid with use of T7 or SP6 mMESSAGE mMACHINE (Ambion, Austin, TX) in the presence of the cap analog m7G(5′)ppp(5′)G (Ambion).

### *Oocyte Preparation and Microinjection*

Oocytes were prepared as previously described (15). Briefly, adult female frogs (*Xenopus laevis*) were anesthetized with 0.3% tricaine (MS-222), and the oocytes were surgically removed from the abdominal incision. The oocytes were placed in ND-96 medium. Oocytes at stage V or VI were subsequently defolliculated in 2 mg/ml collagenase (Sigma Chemical, St. Louis, MO) in $Ca^{2+}$-free OR-2 medium for 80 min at room temperature. The defolliculated oocytes were injected with 46 nl (0.25 μg/μl) of antisense oligonucleotide complementary to endogenous *Xenopus* Cx38: 5′-GCTTTAG-TAATTCCCATCCTGCCATGTTTC-3′ (commencing at nt −5 of Cx38 cDNA sequence) (1) by means of a Nanoject apparatus (Drummond, Broomall, PA). The antisense oligonucleotide blocks completely the endogenous junctional communication within 48 h. At 48–72 h after injection, 46 nl of Cx32 wild-type, tandem, 5R/E, or 5R/N cRNA (0.04, 0.4, 0.46, and 0.2 μg/μl, respectively) were injected into oocytes at the vegetal pole, and the oocytes were incubated overnight at 18°C. The oocytes were mechanically stripped of their vitelline layer in a hypertonic medium (15) and paired at the vegetal poles in ND-96 medium. Oocyte pairs were studied electrophysiologically 2–3 h after pairing.

### *Uncoupling Protocol*

The oocyte chamber was continuously perfused at a flow rate of 0.6 ml/min by a peristaltic pump (Dyamax model RP-1, Rainin Instrument, Woburn, MA). The superfusion solution was ejected by a 22-gauge needle placed near the edge of the conical well containing the oocyte pair. The level of the solution in the chamber was maintained constant by continuous suction. Electrical uncoupling of oocyte pairs was induced by 3–15 min of superfusion (0.6 ml/min) of salines continuously gassed with 100% $CO_2$. A $Cl^-$-free saline ($Cl^-$ replaced with methanesulfonate) was used. The $Cl^-$-free saline contained (in mM) 75 NaOH, 10 KOH, 4 $Ca(OH)_2$, 5 $Mg(OH)_2$, and 10 MOPS, adjusted to pH 7.2 with methanesulfonic acid. As previously reported (15), the opening of $Ca^{2+}$-activated $Cl^-$ channels during exposure to 100% $CO_2$ causes an increase in membrane current that may interfere with measurements of junctional current ($I_j$).

### *Measurement of $G_j$ in Oocyte Pairs*

All the experiments were performed using the standard double-voltage-clamp procedure for measuring $G_j$ (21). After the insertion of a current and a voltage microelectrode in each oocyte, both oocytes were initially voltage clamped to the same holding potential ($V_m$), $V_{m1} = V_{m2}$ (usually −20 mV), so that no $I_j$ would flow at rest ($I_j = 0$). A $V_j$ gradient was created by imposing a +20-mV voltage step ($V_1$) of 2-s duration every 10 or 30 s to *oocyte 1* while maintaining $V_2$ at $V_m$; thus $V_j = V_1$. The negative-feedback current ($I_2$), injected by the clamp amplifier in *oocyte 2* for maintaining $V_2$ constant at $V_m$, was used for calculating $G_j$, inasmuch as it is identical in magnitude to the $I_j$ but of opposite sign ($I_j = -I_2$); $G_j = I_j/V_j$. Pulse generation and data acquisition were performed by means of a computer equipped with pClamp software (Axon Instruments, Foster City, CA) and Labmaster TL-1A/D-D/A interface (Axon).

For studying voltage dependence of $G_j$, each oocyte of the pair was first voltage clamped at −20 mV. Voltage steps of 20 mV (±120 mV maximum) and 20-s duration were then applied every 45 s to either oocyte of the pair while the other was maintained at −20 mV. To illustrate the relationship between steady-state $G_j$ ($G_{jss}$) and $V_j$, the normalized $G_j$ ($G_{jss}/G_{jmax}$, where $G_{jmax}$ is maximum $G_j$) was plotted with respect to $V_j$. The curve was fitted to a two-state Boltzmann distribution of the following form: $(G_{jss} - G_{jmin})/(G_{jmax} - G_{jss}) = \exp[-A(V_j - V_0)]$, where $V_0$ is the $V_j$ value at which the voltage-sensitive conductance is one-half the maximal value, $G_{jmin}$ is the theoretical minimum normalized $G_j$, and $A = nq/kT$ is a constant expressing voltage sensitivity in terms of number of equivalent gating charges ($n$) moving through the entire applied field (where $q$ is the electron charge, $k$ is the Boltzmann constant, and T is the temperature in Kelvin).

## RESULTS

### *Functional Tests of Mutants*

Tandem and 5R/E mutants did not form functional channels when tested homotypically, even after 6–7 h of oocyte pairing. In heterotypic pairs between oocytes expressing tandem or 5R/E and oocytes expressing Cx32 wild type (tandem-32 and 5R/E-32, respectively), coupling developed slowly. Within 2–3 h after pairing, $G_j$ was 0.56 ± 0.14 (SE) μS ($n = 15$) with tandem-32 and 0.34 ± 0.13 μS ($n = 6$) with 5R/E-32. In contrast, 5R/N mutants were functional homotypically (5R/N-5R/N) (26, 28) and heterotypically with Cx32 wild-type mutants (5R/N-32) (27). In 5R/N-32 pairs, $G_j$, measured with the conventional protocol (+20-mV voltage pulses of 2-s duration applied to 1 of the 2 oocytes every 10 s) within 2–3 h after pairing, was 2.03 ± 0.4 μS ($n = 19$). In homotypic 5R/N-5R/N and 32–32 pairs, $G_j$ was 3.8 ± 1.3 ($n = 8$) and 4.2 ± 1.3 μS ($n = 26$), respectively.

### *Sensitivity to $V_j$ Pulses*

*Tandem-32 channels.* Cx32 junctions displayed a characteristic sensitivity to $V_j$. As shown in Fig. 1*A*, $I_j$

decayed exponentially with time for $V_j > \pm 40$ mV. In contrast, tandem-32 channels displayed a unique $I_j$-$V_j$ behavior (Fig. 1*A*). With the tandem side negative, as $V_j$ was increased in 20-mV steps from 20 to 120 mV, the initial and final $I_j$ progressively decreased to very low conductance values, and the channels appeared to be $V_j$ sensitive even at the lowest $V_j$. With the tandem side positive, as $V_j$ increased in steps from 20 to 120 mV, $I_j$ progressively increased to high values, and $I_j$ recorded at the end of the pulse was greater than the initial $I_j$, as if $V_j$ caused an increase rather than a decrease in $I_j$. Only at the largest $V_j$ gradients (100–120 mV), two fairly conventional $I_j$ levels started to appear (Fig. 1*A*). The asymmetric $I_j$-$V_j$ behavior of tandem-32 and other heterotypic mutant-32 junctions is clearly demonstrated by plotting normalized $G_j$ ($G_{jss}/G_{jmax}$) vs. $V_j$ (Fig. 1, *C* and *D*).

This intriguing voltage behavior seemed to suggest that $V_j$ gradients that made the tandem side of the channels negative or positive progressively closed or opened, respectively, an increasing number of channels. A channel population out of steady state would obviously mask the normal $V_j$ behavior of individual channels, generating the false impression of increased $V_j$ sensitivity with the tandem side negative and the absence of $V_j$ sensitivity with the tandem side positive, up to the time when all the channels had opened.

To test this idea, trains of 60-mV $V_j$ pulses (tandem side positive) of 20-s duration (45-s intervals) were applied and immediately followed by the conventional $V_j$ protocol (tandem side positive). Three distinct $I_j$ behaviors were observed during the train of 60-mV pulses (Fig. 1*B*): a monophasic $I_j$ increase (*pulses 1–3*); a biphasic $I_j$ time course (*pulses 4–9*), characterized by an initial progressive $I_j$ increase followed by an exponential $I_j$ decay; and a conventional $I_j$ behavior (*pulses 10–18*), depicted by an initial $I_j$ peak followed by an exponential $I_j$ decay to a steady-state level. After the train of $V_j$ pulses, the application of conventional $V_j$ protocols (tandem side positive) resulted in a current behavior relatively similar to that of 32–32 channels. However, note in Fig. 1*B* that *pulse 21* ($V_j$ = 60 mV) generated a biphasic $I_j$ time course similar to that of *pulse 6*, suggesting that, after the end of the train of 60-mV $V_j$ pulses, some of the channels might have closed.

*5R/E-32 channels.* 5R/E-32 channels subjected to the conventional $V_j$ protocol behaved as tandem-32 channels (Fig. 1*A*). With the 5R/E side negative, initial and final $I_j$ progressively decreased to very low values, and the channels appeared to be $V_j$ sensitive even at the lowest $V_j$. With the 5R/E side positive, $I_j$ progressively increased to very high values, and with $V_j$ gradients as high as 80 mV $I_j$ measured at the end of the pulse was greater than the initial $I_j$. Only with the largest $V_j$ gradients (100–120 mV) did two fairly conventional $I_j$ levels start to appear (Fig. 1*A*). As for tandem-32 channels, the relationship between normalized $G_j$ ($G_{jss}/G_{jmax}$) and $V_j$ clearly demonstrates the asymmetric $I_j$-$V_j$ behavior of 5R/E-32 junctions (Fig. 1*D*).

*5R/N-32 channels.* The behavior of 5R/N-32 channels exposed to the conventional $V_j$ protocol was not as asymmetric as that of tandem-32 or 5R/E-32 channels (Fig. 1*A*). With $V_j > 20$ mV, initial and final $I_j$ were higher with the 5R/N side positive than negative at each comparable $V_j$ value (Fig. 1*A*). This moderate asymmetry is displayed in Fig. 1*C*, which plots the normalized $G_j$ ($G_{jss}/G_{jmax}$) vs. $V_j$ and the two-state Boltzmann fit for 5R/N-32 and 32–32 channels. The Boltzmann values of 5R/N-32 channels are as follows: $V_0$ = 52.6 mV, $n$ = 2.4, and $G_{jmin}$ = 0.11 ($n$ = 3) for the 5R/N side negative and $V_0$ = 77.2 mV, $n$ = 2.4, and $G_{jmin}$ = 0.22 ($n$ = 3) for the 5R/N side positive. Those of homotypic 32–32 and 5R/N-5R/N channels are similar: $V_0$ = 59.5 mV, $n$ = 2.1, and $G_{jmin}$ = 0.29 ($n$ = 7) and $V_0$ = 59.8 mV, $n$ = 2.3, and $G_{jmin}$ = 0.21 ($n$ = 5), respectively. On the basis of data described below, the asymmetric voltage behavior of mutant-32 channels may indicate that progressive exposure to prolonged $V_j$ gradients that make the mutant side negative or positive progressively closes or opens, respectively, an increasing number of channels.

### *Effect on $G_j$ of Trains of Long $V_j$ Pulses*

The asymmetric $I_j$-$V_j$ behavior of mutant-32 channels (Fig. 1*A*) suggested that $V_j$-dependent channel opening and closing processes might have a long time constant ($\tau$), possibly reflecting the function of a "slow gate," distinct from the conventional, relatively fast, $V_j$-sensitive gate. To further test this idea, $G_j$ was measured immediately before and after the application of trains of $V_j$ pulses (60 mV, 20 s) with the mutant side positive and then negative (Fig. 2).

*Tandem-32 channels.* With $V_j$ pulses positive at the tandem side, $I_j$ behaved as previously described (cf. Fig. 2*A*, *left trace*, with Fig. 1*B*). With the tandem side negative, initial and final $I_j$ levels progressively decreased to very low values (Fig. 2*A*, *right trace*). $G_j$, measured with the conventional protocol (+20-mV pulses of 2-s duration applied to 1 oocyte every 10 s) immediately after the train of $V_j$ pulses positive at the tandem side (*pulse train 1*), was 130% greater than that measured before the train of $V_j$ pulses (Fig. 2*B*) and recovered in 3–4 min (Fig. 2*B*). $G_j$ measured immediately after the train of 60-mV $V_j$ pulses (*pulse train 2*) negative at the tandem side decreased to 23% of control values (Fig. 2*B*). This behavior suggested $V_j$-dependent channel opening and closing processes, with long time constants, that could reflect the function of a slow $V_j$-sensitive gate.

*5R/E-32 channels.* 5R/E-32 channels displayed a similar $I_j$ behavior (Fig. 2*C*) but, with the 5R/E side positive, only the first pulse resulted in a monophasic $I_j$ increase, whereas subsequent pulses progressively assumed a more conventional $I_j$ behavior: an initial $I_j$ peak followed by exponential $I_j$ decay (Fig. 2*C*, *left trace*). However, initial and final $I_j$ levels increased exponentially over the first six to seven pulses (Fig. 2*C*, *left trace*). With the 5R/E side negative, initial and final $I_j$ levels progressively decreased to very low conductance values (Fig. 2*C*, *right trace*). $G_j$ increased by 110%

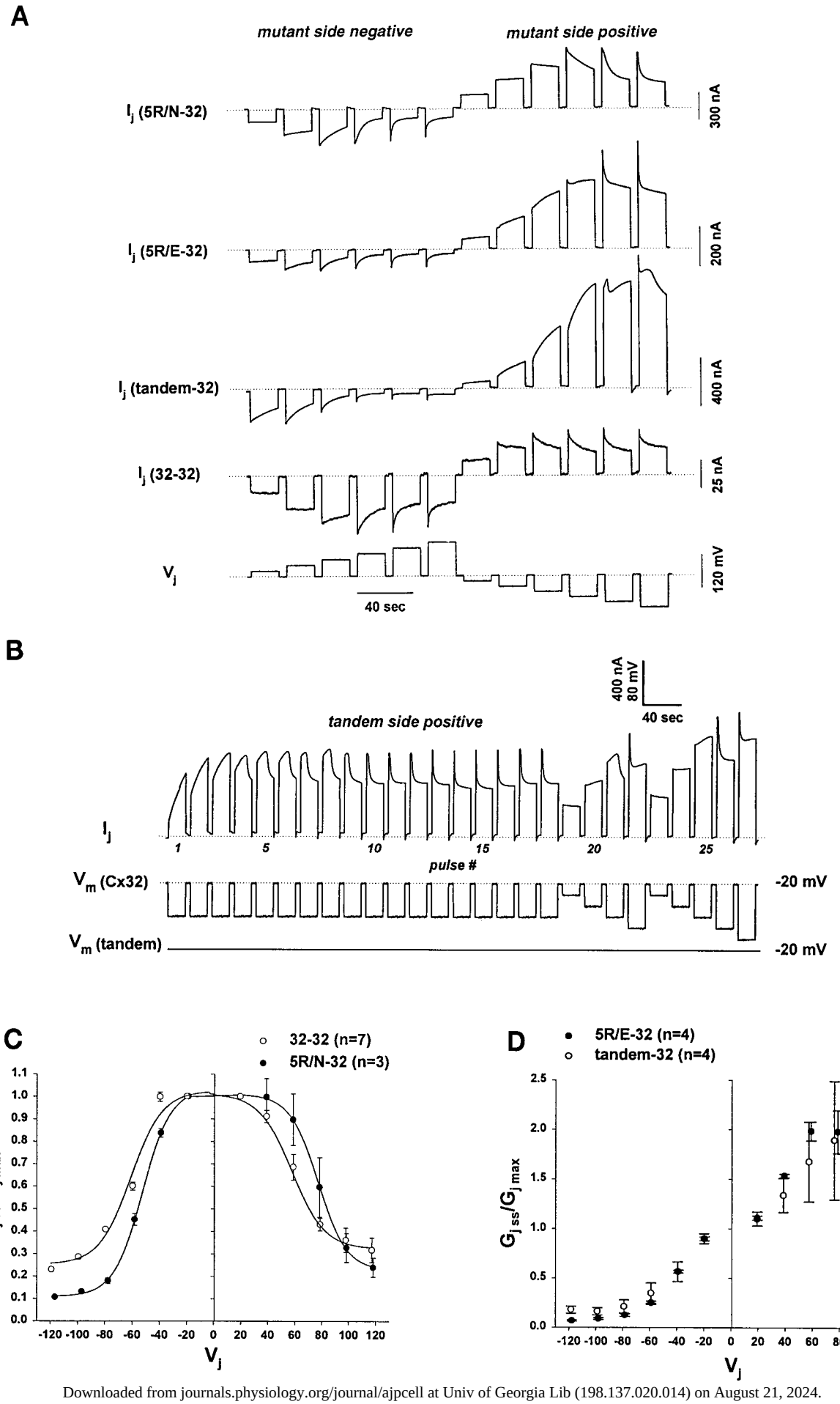

during the train of $V_j$ pulses (*pulse train 1*) positive at the 5R/E side (Fig. 2*D*) and recovered exponentially in 4–5 min (Fig. 2*D*). In contrast, $G_j$ reversibly dropped to 31% of control values with pulses (*pulse train 2*) negative at the 5R/E side (Fig. 2*D*).

*5R/N-32 channels.* 5R/N-32 channels displayed an $I_j$ behavior (Fig. 2*E*) qualitatively similar to that of tandem-32 (Fig. 2*A*) and 5R/E-32 (Fig. 2*C*) channels. With the 5R/N side positive, the first pulse resulted in a monophasic $I_j$ increase from initial to final $I_j$, whereas subsequent pulses generated a more conventional $I_j$ behavior: an initial $I_j$ peak followed by exponential $I_j$ decay (Fig. 2*E*, *left trace*). Initial and final $I_j$ levels increased sizably between the first and the second pulse but only slightly with subsequent pulses (Fig. 2*E*, *left trace*). In contrast, with the 5R/N side negative, initial and final $I_j$ levels progressively decreased to lower conductance values (Fig. 2*E*, *right trace*). $G_j$ increased by 11% during the application of the train of $V_j$ pulses (*pulse train 1*) positive at the 5R/N side (Fig. 2*F*) and recovered to control values in 4–5 min (Fig. 2*F*). In contrast, $G_j$ reversibly dropped to 63% of control values with pulses (*pulse train 2*) negative at the 5R/N side (Fig. 2*F*).

*32–32 channels.* The application of similar trains of $V_j$ pulses of either polarity to homotypic 32–32 channels (Fig. 2*G*) caused a small and reversible $G_j$ drop to ~90% of control values (Fig. 2*H*). This indicates that, albeit to a lesser extent, repeated $V_j$ pulses affect a slow $V_j$-sensitive gate in homotypic Cx32 wild-type channels as well.

### *Effect on $G_j$ of Steady-State $V_j$*

The ability of trains of long $V_j$ pulses of opposite polarity to progressively increase or decrease $G_j$ in tandem-32, 5R/E-32, and 5R/N-32 junctions suggested that these channels might also be sensitive to prolonged, steady-state $V_j$ gradients. If so, steady-state $V_j$ protocols could enable one to better define the magnitude and kinetics of this process.

*Tandem-32 channels.* In oocyte pairs in which each oocyte was initially clamped at $V_m = -20$ mV ($V_j = 0$), the establishment of steady-state $V_j = 40$ mV (tandem side positive) increased $G_j$ exponentially by 262 ± 64% (mean ± SD, $n = 4$), with $\tau = 0.88 \pm 0.2$ (SD) min ($n = 4$; Fig. 3*A* and *B*); $G_j$ was measured by the conventional protocol: +20-mV pulses of 2-s duration applied to one oocyte every 10 s. Similar results were obtained by simultaneously depolarizing the tandem side and hyperpolarizing the Cx32 side or by just hyperpolarizing the Cx32 side in oocytes initially clamped at −20 mV (Fig. 3*A* and *B*) or −40 mV. $V_j$ gradients of 10 and 20 mV increased $G_j$ by 10–20% and 80–130%, respectively (data not shown).

In experiments in which oocytes initially clamped at $V_j = 0$ mV were subjected to $V_j = 60$ mV (tandem side positive), $G_j$ increased exponentially by 581 ± 278% (mean ± SD, $n = 4$), with $\tau = 1.3 \pm 0.4$ (SD) min ($n = 4$). With the reestablishment of $V_j = 0$ mV from $V_j$ (tandem side positive) = 40 mV (Fig. 3*A*) or 60 mV, $G_j$ decreased slowly after a single-exponential decay, with $\tau = 1.6 \pm 0.2$ min ($n = 3$). After the application of $V_j = 40$–60 mV (tandem side positive), $G_j$ did not return to baseline values even after 7–8 min (Fig. 3*A*), indicating that channels opened by positive $V_j$ gradients closed very slowly. In contrast, when $V_j$ was reversed from tandem side positive to tandem side negative, $G_j$ decreased more rapidly and dramatically (Fig. 3*B*). With $V_j$ reversal to 40 or 60 mV (tandem side negative), $G_j$ decreased to 16 ± 11% ($n = 4$) or ~0% of control values (measured at $V_j = 0$) after exponential decays, with $\tau = 0.4 \pm 0.16$ min ($n = 4$), indicating that the relative negativity of the tandem side actively closed the channels.

Interestingly, on return to $V_j = 0$ mV from $V_j = 40$ mV (Fig. 3*A*) or 60 mV, tandem side positive, $G_j$ increased abruptly, then dropped. This is due to the reopening of the conventional (fast) $V_j$-sensitive gate. This interpretation is also supported by the observation that the abrupt increase in $G_j$ is not observed when $V_j$ is reversed from positive to negative at the tandem side (Fig. 3*B*); in this case, as the conventional $V_j$ gates open at the Cx32 side, they close at the mutant side, or vice versa.

*5R/E-32 channels.* Similar results were obtained with 5R/E-32 channels. Exposure to $V_j = 40$ mV (5R/E

Fig. 1. Response of junctional current ($I_j$) to transjunctional voltage ($V_j$) pulses in *Xenopus* oocyte pairs expressing homotypic Cx32 channels (32–32, *A*) or heterotypic channels between Cx32 wild-type and tandem (tandem-32, *A* and *B*), 5R/E (5R/E-32, *A*), or 5R/N (5R/N-32, *A*). 32–32 channels (*A*) display a characteristic sensitivity to $V_j$, as $I_j$ decays exponentially with time for *V*j greater than ±40 mV. In contrast, tandem-32 and 5R/E-32 channels (*A*) display a unique $I_j$-$V_j$ behavior (*A*). With mutant side negative (*A, left*), as $V_j$ is increased from 20 to 120 mV, initial and final $I_j$ progressively decrease to very low values, and $V_j$ sensitivity seems present even at $V_j = 20$ mV. With mutant side positive (*A, right*), $I_j$ progressively increases to high values, and $I_j$ increases, rather than decreases, from initial $I_j$; only with $V_j = 100$–120 mV, 2 more conventional $I_j$ levels are seen. With trains of 60-mV $V_j$ pulses (tandem side positive), 3 distinct $I_j$ behaviors are observed: a monophasic increase in $I_j$ (*B, pulses 1–3*); a biphasic $I_j$ time course (*B, pulses 4–9*), with initial $I_j$ increase followed by exponential $I_j$ decay; and, finally, a conventional $I_j$ behavior (*B, pulses 10–18*). Subsequent applications of conventional $V_j$ protocol (tandem side positive) result in fairly conventional $I_j$ behaviors (*B, pulses 19–27*). *Pulse 21* generates a biphasic $I_j$ time course, as does *pulse 6*, suggesting that some channels had closed after 60-mV pulses. Behavior of 5R/N-32 channels is qualitatively similar but not as asymmetric as that of tandem-32 or 5R/E-32 channels (*A*). With $V_j > 20$ mV, initial and final $I_j$ are higher with positive (*A, right*) than with negative (*A, left*) $V_j$. *C* and *D*: asymmetric $I_j$-$V_j$ behavior of tandem-32 and other heterotypic mutant-32 junctions is demonstrated by plots of normalized $G_j$ ($G_{jss}/G_{jmax}$, where $G_{jss}$ is steady-state $G_j$ and $G_{jmax}$ is maximum $G_j$) vs. $V_j$. *C*: 2-state Boltzmann fit for 5R/N-32 and 32–32 channels. Boltzmann values are $V_0 = 52.6$ mV, $n = 2.4$, and minimum $G_j$ ($G_{jmin}$) = 0.11 ($n = 3$) with 5R/N side negative (*C, left*) and $V_0 = 77.2$ mV, $n = 2.4$, and $G_{jmin} = 0.22$ ($n = 3$) with 5R/N side positive (*C, right*) for 5R/N-32 channels and $V_0 = 59.5$ mV, $n = 2.1$, and $G_{jmin} = 0.29$ for 32–32 channels.

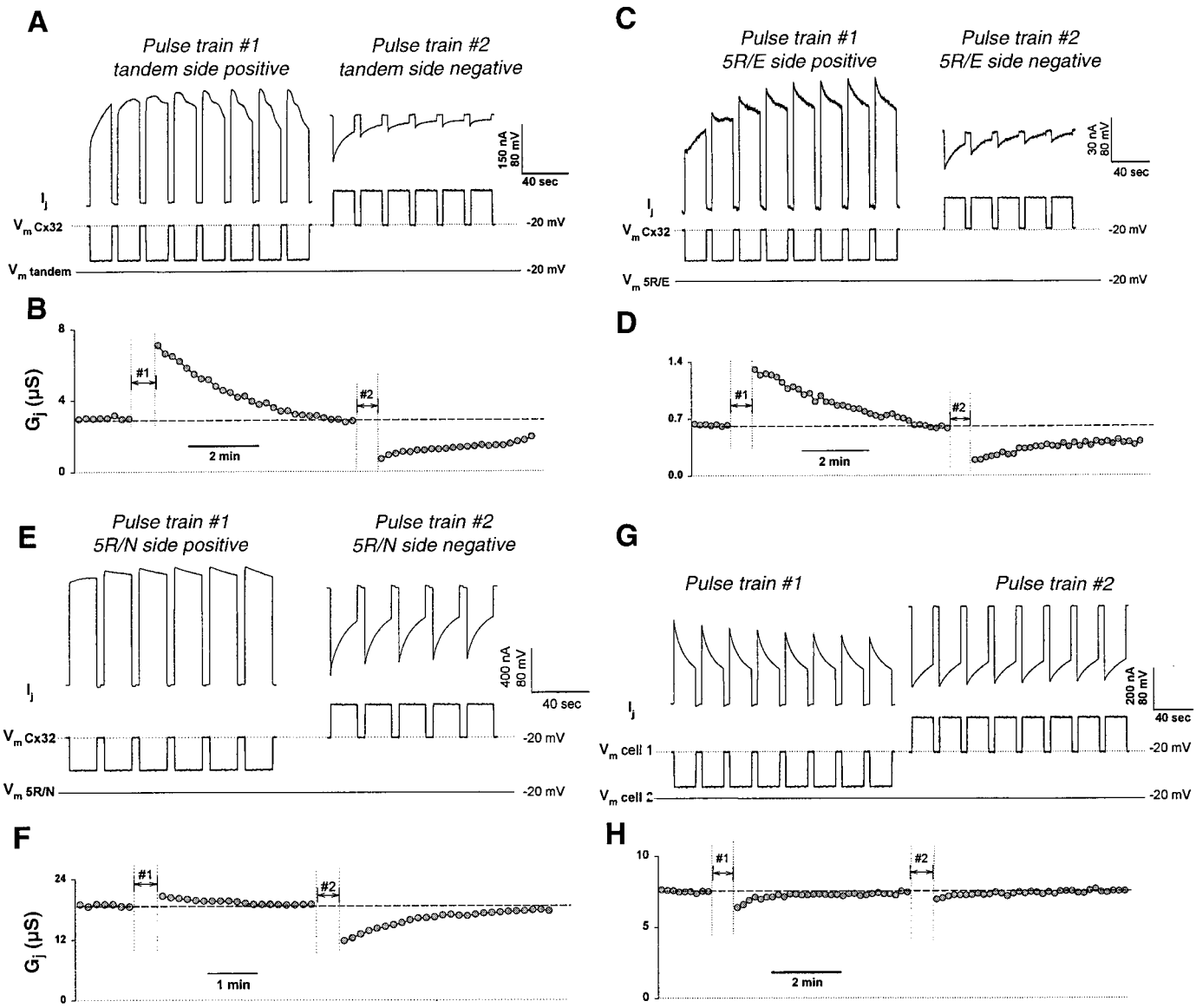


Fig. 2. Effect on $G_j$ of trains of long $V_j$ pulses of opposite polarity (*A*, *C*, *E*, and *G*). $G_j$ of tandem-32 (*B*), 5R/E-32 (*D*), 5R/N-32 (*F*), and 32–32 (*H*) channels was measured with conventional protocol: +20-mV pulses of 2-s duration applied to 1 oocyte every 10 s ($V_j$ = 20 mV during pulse, $V_j$ = 0 mV between pulses) immediately before and after trains of $V_j$ pulses (60 mV, 20-s duration, every 45 s) with mutant side positive (*A*, *C*, and *E*, *left traces*) or negative (*A*, *C*, and *E*, *right traces*). With tandem side positive, $I_j$ behaves as previously described (cf, *A*, *left trace*, with Fig. 1*B*). With tandem side negative, initial and final $I_j$ progressively decrease to low values (*A*, *right trace*). $G_j$ increases by 130% with train of $V_j$ pulses (*pulse train 1*) that make tandem side positive (*B*) and recovers exponentially in 3–4 min (*B*). In contrast, $G_j$ reversibly decreases to 23% of control values with pulses (*pulse train 2*) negative at tandem side (*B*). A similar behavior is observed with 5R/E-32 channels (*C* and *D*). With 5R/E side positive, 1st pulse causes a monophasic $I_j$ increase, whereas subsequent pulses progressively assume a more conventional $I_j$ behavior (*C*). Initial and final $I_j$ levels increase exponentially over 1st 6–7 pulses (*C*, *left trace*). With 5R/E side negative, initial (instantaneous) and final $I_j$ levels progressively decrease to very low values (*C*, *right trace*). $G_j$ increases by 110% with $V_j$ pulses (*pulse train 1*) positive at 5R/E side (*D*) and recovers exponentially in 4–5 min (*D*). In contrast, $G_j$ drops to 31% of control values with pulses (*pulse train 2*) negative at 5R/E side (*D*). 5R/N-32 channels (*E* and *F*) behave qualitatively as tandem-32 and 5R/E-32 channels, but not as dramatically. With 5R/N side positive, 1st pulse results in a monophasic $I_j$ increase, whereas subsequent pulses generate a more conventional $I_j$ behavior (*E*, *left trace*). Initial and final $I_j$ levels increase sizably between 1st and 2nd pulse, but only slightly with subsequent pulses (*E*, *left trace*). In contrast, with 5R/N side negative, both $I_j$ levels progressively decrease to lower values (*E*, *right trace*). $G_j$ increases by 11% with $V_j$ pulses (*pulse train 1*) positive at 5R/N side (*F*) and recovers exponentially in 4–5 min (*F*), whereas $G_j$ reversibly drops to 63% of control values with pulses (*pulse train 2*) negative at 5R/N side (*F*). In contrast, trains of 60-mV $V_j$ pulses of either polarity applied to homotypic 32–32 channels (*G*) reversibly decrease $G_j$ to ~90% of control values (*H*).

side positive) increased $G_j$ by 182 ± 50% (mean ± SD, $n = 5$), with $\tau = 1.28 \pm 0.33$ (SD) min ($n = 5$; Fig. 3, *C* and *D*). $G_j$ increased by as much as 400% with $V_j = 60$ mV. On return to $V_j = 0$ mV, $G_j$ recovered slowly (Fig. 3*C*), with $\tau = 2.04 \pm 0.35$ min ($n = 4$). When $V_j$ was reversed from positive to negative at the 5R/E side, $G_j$ drastically decreased (Fig. 3*D*) to 14.8 ± 3.3% ($n = 4$) of control values (measured at $V_j = 0$), with $\tau = 0.39 \pm 0.07$ min ($n = 4$). As for tandem-32 channels, on return to $V_j = 0$ mV from $V_j = 40$ mV (5R/E side positive), $G_j$ increased abruptly before dropping (Fig. 3*C*) because of the reopening of conventional $V_j$-sensitive gates. Indeed, as expected, this abrupt increase in $G_j$ was not observed when the $V_j$ polarity was reversed from positive to negative (Fig. 3*D*).

*5R/N-32 channels.* 5R/N-32 channels behaved qualitatively as tandem-32 and 5R/E-32 channels. The establishment of $V_j = 40$ mV (5R/N side positive) increased $G_j$ reversibly and exponentially by 23 ± 19.5% (mean ± SD, $n = 18$; Fig. 3, *E* and *F*), with $\tau = 0.78 \pm 0.32$ (SD) min ($n = 11$). With reestablishment of $V_j = 0$ mV, $G_j$ recovered, with $\tau = 2.4 \pm 0.9$ min ($n = 4$). When the channels were subjected to $V_j$ negative at the 5R/N side from $V_j = 0$ mV (Fig. 3*E*) or $V_j = 40$ mV (5R/N side positive; Fig. 3*F*), $G_j$ dropped to 35.2 ± 17.3% ($n = 10$) of control values (measured at $V_j = 0$), with $\tau = 1.05 \pm 0.61$ min ($n = 9$). On return to $V_j = 0$ mV from $V_j = 40$ mV, 5R/N side positive, $G_j$ increased abruptly, then dropped (Fig. 3*E*); this was not observed with $V_j$ reversal from positive to negative (Fig. 3*F*), as described for tandem-32 (Fig. 3*B*) and 5R/E-32 (Fig. 3*D*) channels.

*32–32 channels.* In homotypic 32–32 junctions the application of 40-mV $V_j$ gradients to either oocyte decreased $G_j$ to 67.7 ± 8.2% (mean ± SD, $n = 7$; Fig. 3*G*). On $V_j$ application, $G_j$ dropped rapidly in the first 10–20 s (Fig. 3*G*, more obvious with 1st $V_j$ application) and then slowly over the following 4–5 min, eventually reaching a steady-state value. The rapid drop and the slow decay may result from the sequential closures of the conventional (fast) $V_j$ gate and the slow $V_j$ gate, respectively.

### *Effect of Simultaneous Depolarization or Hyperpolarization of Both Oocytes*

The heterotypic channels were tested for sensitivity to $V_m$ by depolarizing or hyperpolarizing both oocytes in 20-mV steps starting from $V_m = -20$ mV ($V_{m1} = V_{m2}$, $V_j = 0$). Neither depolarizations as great as $V_m = +20$ mV nor hyperpolarizations as high as $V_m = -60$ mV had any effect on $G_j$ (Fig. 3*H*), indicating that tandem-32 channels, like other vertebrate cell-cell channels, are insensitive to $V_m$, the voltage between the inside and the outside of the cell. The same results were obtained with the other mutant-32 channels and with homotypic 32–32 and 5R/N-5R/N channels (data not shown). $V_m$ sensitivity is present in insect gap junctions (11), whereas connexins, with the possible exception of Cx26 (1), are insensitive to $V_m$.

### *$CO_2$ Sensitivity*

Homotypic 32–32 channels were weakly sensitive to $CO_2$, as previously reported (22). $G_j$ decreased to 85 ± 5% (mean ± SE, $n = 7$) with a 3-min exposure to $CO_2$ (Fig. 4*A*) and to 47 ± 4.8% with a 15-min exposure ($n = 16$; Fig. 4*B*) at a maximum rate of ~9%/min. Tandem-32 channels were more sensitive to $CO_2$ than 32–32 channels. $G_j$ dropped to 43 ± 8% ($n = 5$) with 3-min exposures to $CO_2$ (Fig. 4) and to 6.4 ± 5% ($n = 4$) with 15-min exposures (Fig. 4*B*) at a maximum rate of ~13%/min. 5R/E-32 channels were much more sensitive to $CO_2$ than 32–32 channels (Fig. 4). $G_j$ dropped to zero ($n = 3$) with 3-min exposures to $CO_2$ at a maximum rate of ~37%/min (Fig. 4).

As previously reported (26), the sensitivity of 5R/N-32 channels was also greater than that of 32–32 channels. $G_j$ decreased to 37.5 ± 6.4% (mean ± SE, $n = 3$) with 3-min exposures to $CO_2$ (Fig. 4*B*) and to ~0% ($n = 4$) with 15-min exposures (Fig. 4*B*) at a maximum rate of ~21%/min. Thus the $CO_2$ sensitivity of all these channels ranked as follows: 5R/E-32 > 5R/N-32 > tandem-32 > 32–32.

### *Effect on $G_j$ of Steady-State $V_j$ During $CO_2$-Induced Uncoupling*

Oocyte pairs expressing mutant-32 or 32–32 channels were subjected to $V_j$ gradients of different polarity during exposure to 100% $CO_2$. In mutant-32 channels, $G_j$, reduced to very low values by exposure to $CO_2$ at $V_j = 0$ mV, increased dramatically and reversibly with $V_j$ gradients that made the tandem (Fig. 5*A*), 5R/E (Fig. 5*C*), or 5R/N (Fig. 5*D*) side positive by 40 mV. Similar results were obtained by simultaneously depolarizing the mutant side and hyperpolarizing the Cx32 side or by just hyperpolarizing the Cx32 side (Fig. 5, *A*, *C*, and *D*). With the same $V_j$ gradient, $G_j$ increased more during uncoupling or recovery from uncoupling than during maximal uncoupling. This was most obvious with 5R/E-32 channels (Fig. 5*C*), inasmuch as their $CO_2$ sensitivity is so high that $G_j$ remains 0 μS for several minutes even with $CO_2$ exposures as short as 3–5 min (Figs. 4*A* and 5*C*). With tandem-32, 5R/E-32, and 5R/N-32 channels, the application of $V_j = 40$ mV (mutant side positive) during $CO_2$ uncoupling (Fig. 5, *A*, *C*, and *D*) increased $G_j$ by ~1,000, ~2,600, and ~600%, respectively. This is noteworthy, because in the absence of $CO_2$, similar $V_j$ applications increased $G_j$ by only ~260, ~180, and ~23%, respectively (see above). These data indicated that $V_j$ is able to open tandem-32, 5R/E-32, and 5R/N-32 channels that had been closed by the $CO_2$ treatment. In contrast, $V_j$ gradients that made the mutant side negative dramatically and reversibly reduced $G_j$ to very low values (Fig. 5, *A*, *C*, and *D*). When a similar protocol was tested on 32–32 channels, the application of 40-mV $V_j$ gradients of either polarity always resulted in a significant drop of $G_j$ (Fig. 5*B*). The magnitude of the $G_j$ drop indicates that also in the case of 32–32 channels $V_j$ affects the conventional $V_j$ gate and the slow $V_j$ gate.

## DISCUSSION

This study shows that oocytes expressing tandem, 5R/E, or 5R/N mutants have altered sensitivity to $CO_2$ and $V_j$ when paired with oocytes expressing Cx32 wild-type mutants. When $V_j$ is depolarized with respect to the mutant-expressing oocyte, $G_j$ increases rather than decreases. Positive $V_j$ at the mutant side is also effective in reopening channels closed by 100% $CO_2$.

Tandem and 5R/E mutants did not display functional channels in homotypic configuration. A possibility is that tandem and 5R/E mutants assume conformations unsuitable for homotypic interaction. In the tandem mutant the $NH_2$-to-COOH terminus linkage may render opposite dimers too rigid for interaction but able to interact heterotypically with more flexible Cx32 monomers. However, the architecture of tandems in connexons is difficult to predict, and in the absence of structural information the possibility that only one of the two monomers of a tandem is normally inserted in the membrane cannot be discounted.

In tandem-32 and 5R/E-32 pairs, $G_j$ is low when measured at $V_j = 0$ mV but increases dramatically with depolarization of the mutant-expressing oocyte. This large increase in $G_j$ with positive $V_j$ at the mutant side

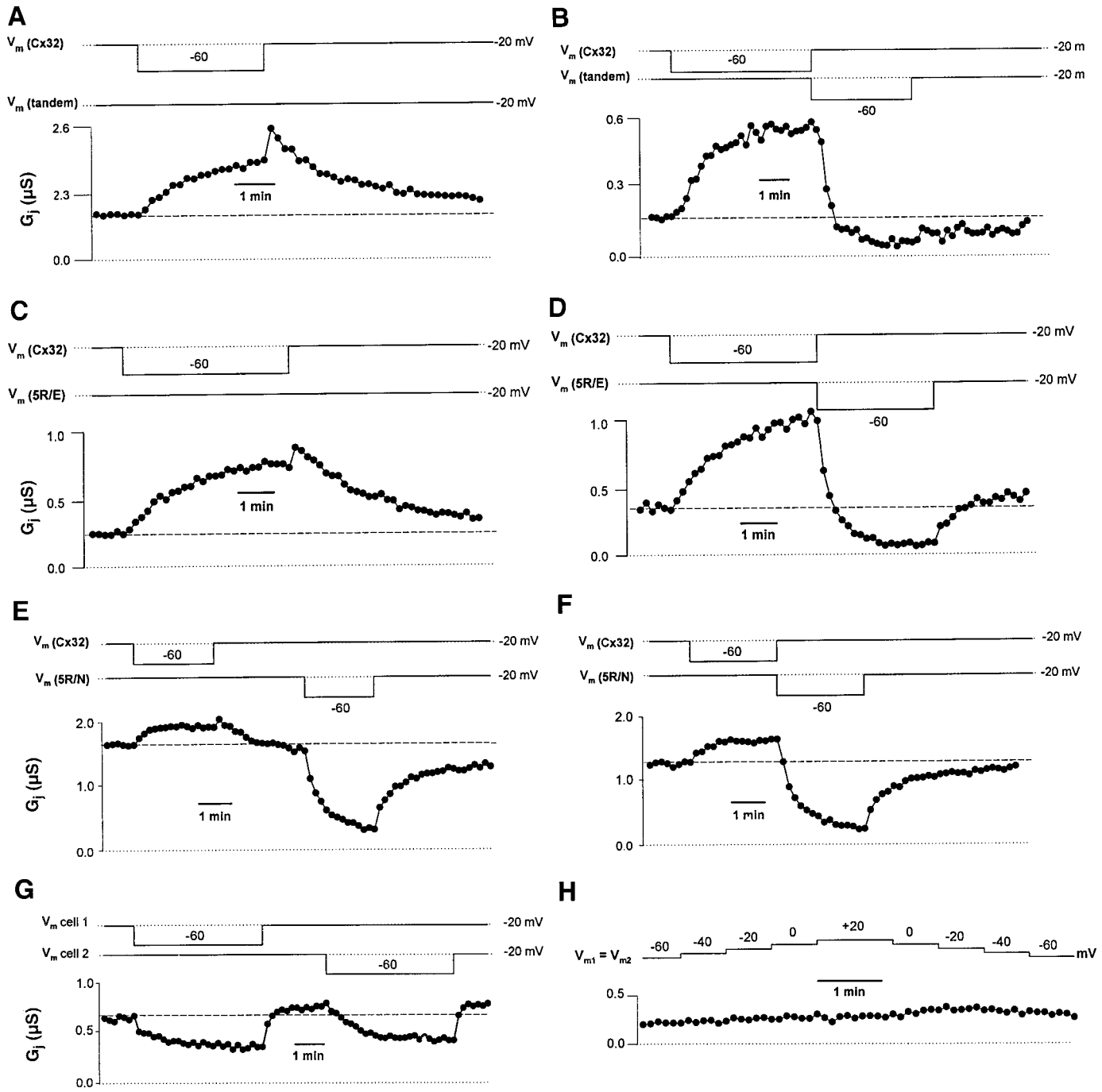

could be explained in a number of ways: new channel formation, increase in single-channel open probability ($P_o$), increase in single-channel conductance ($\gamma_j$), or a combination of the above. Although it is possible that positive $V_j$ favors channel formation, this is considered unlikely, because it would mean that channels formed by positive $V_j$ at the mutant side are removed on return to $V_j = 0$ mV and that negative $V_j$ at the mutant side removes newly formed and preexisting channels. One would have to assume that channel formation and removal are based on the same mechanism, which is unlikely. Because $G_j$ measured at $V_j = 0$ mV did not significantly increase after the first 2–3 h of pairing, we believed that at that time the channel population had reached some stability, at least in terms of new channel formation.

Whether the observed phenomenon is due to changes in $P_o$ and/or $\gamma_j$ can only be determined at the single-channel level. Interestingly, $\gamma_j$ was found to be sensitive to $V_j$ in heterotypic Cx32/Cx26 channels (4). However, in this case, even $V_j$ as high as ±100 mV did not change $\gamma_j$ by >50% in either direction, whereas in our case $V_j$ as low as 40 mV (tandem or 5R/E side positive) increased $G_j$ by as much as two- to threefold and $V_j$ as low as 60 mV (tandem or 5R/E side negative) reduced $G_j$ to nearly zero. Therefore, this is likely to be a gating phenomenon involving changes in $P_o$. Tandem, 5R/E, and 5R/N mutants may display the function of a slow, $V_j$-sensitive gate.

If it is assumed that this is a channel gating phenomenon, does it involve the conventional $V_j$-sensitive gate or another gate, a slow gate? Several elements suggest that we might be dealing with a slow gate distinct from the conventional $V_j$ gate. The presumed slow gates appear to open and close with time constants on the order of minutes, whereas $V_j$ gates close with time constants of a few seconds. $V_j$ gradients of 40–60 mV (mutant side negative) close most of the channels, whereas even with $V_j$ gradients of ±120 mV a 20–25% residual conductance is usually observed (5). Even a $V_j$ gradient as low as 10 mV (tandem side positive) significantly increases $G_j$, whereas the conventional $V_j$-sensitive gate is insensitive to $V_j < 20$–40 mV. Furthermore, the distinct behavior of the two gates is clearly manifested by the abrupt increase in $G_j$ observed with return to $V_j = 0$ mV from positive $V_j$ at the mutant side (Fig. 3, *A*, *C*, and *E*). Because the conventional $V_j$ gate of Cx32 is believed to close with negative potentials (22), the abrupt increase in $G_j$ is likely to mark the reopening of some of the Cx32 $V_j$ gates. This interpretation is further confirmed by the observation that this abrupt increase in $G_j$ is absent when $V_j$ is reversed from positive to negative at the mutant side; in this case, the behavior of the conventional $V_j$ gate is masked, because, with $V_j$ reversal, whereas the $V_j$ gate of the Cx32 hemichannel opens that of the mutant hemichannel closes, or vice versa. Recently, additional evidence for a distinction between a slow gate and a conventional $V_j$ gate has come from our preliminary data (unpublished observations) on the behavior of heterotypic channels between Cx26 wild-type and Cx26 mutant (4basic/E) channels, in which, as in 5R/E, all four basic residues of CT were mutated to E (R215E, K220E, K222E, and R223E). Interestingly, these channels behaved qualitatively as 5R/E-32 channels when exposed to $V_j$ in the presence and absence of $CO_2$, despite the fact that the conventional (fast) $V_j$ gates of Cx26 and Cx32 are sensitive to opposite voltage polarities (22).

Is the slow gate active in wild-type connexins as well? In homotypic 32–32 channels, exposure to steady-state $V_j$ (40 mV) of either polarity decreased $G_j$ to ~68%. The time course of $G_j$ decay had a fast and a slow component, suggesting that also in these channels fast and slow $V_j$ gates are activated. However, with 32–32 channels the $G_j$ drop was much smaller than with mutant-32 channels, indicating that the effect of negative $V_j$ on the slow gate is less pronounced in wild-type Cx32 than in mutant hemichannels.

Most intriguing is the observation that $V_j$ gradients (mutant side positive) significantly increase $G_j$ in oocytes partially or totally uncoupled by $CO_2$. This raises the possibility that the chemical gate is voltage sensitive and that the chemical gate and the slow gate are

Fig. 3. $G_j$ response to steady-state $V_j$ gradients in tandem-32 (*A* and *B*), 5R/E-32 (*C* and *D*), 5R/N-32 (*E* and *F*), and 32–32 (*G*) channels and to holding potential ($V_m$) in tandem-32 channels (*H*); $G_j$ was measured by usual pulse protocol (+20-mV voltage pulses of 2-s duration applied to 1 oocyte every 10 s). In oocytes initially clamped at $V_m = -20$ mV ($V_j = 0$), a 40-mV $V_j$ step (tandem side positive) exponentially increases $G_j$ by 262 ± 64% (mean ± SD, $n = 4$), with $\tau = 0.88 \pm 0.2$ (SD) min ($n = 4$), in tandem-32 channels (*A* and *B*). On return to $V_j = 0$ mV from $V_j = 40$ mV (*A*) tandem side positive, $G_j$ decreases exponentially, with $\tau = 1.6 \pm 0.2$ min ($n = 3$), but does not reach baseline (control) values even after 7–8 min. With $V_j$ reversal to 40 mV (tandem side negative), $G_j$ decreases exponentially to 16 ± 11% ($n = 4$) (*B*) of control values with $\tau = 0.4 \pm 0.16$ min ($n = 4$), indicating that relative negativity of tandem side actively closes channels. 5R/E-32 channels behave similarly (*C* and *D*). Exposure to $V_j = 40$ mV (5R/E side positive) increases $G_j$ by 182 ± 50% ($n = 5$), with $\tau = 1.28 \pm 0.33$ min ($n = 5$, *C* and *D*). With return to $V_j = 0$ mV, $G_j$ recovers slowly to control values (*C*), with $\tau = 2.04 \pm 0.35$ min ($n = 4$). With $V_j$ reversal from positive to negative, $G_j$ decreases (*D*) to 14.8 ± 3.3% ($n = 4$) of control values (measured at $V_j = 0$), with $\tau = 0.39 \pm 0.07$ min ($n = 4$). 5R/N-32 channels behave qualitatively as tandem-32 and 5R/E-32 channels, but $G_j$ fluctuations are less dramatic (*E* and *F*). Establishment of $V_j = 40$ mV (5R/N side positive) increases $G_j$ by 23 ± 19.5% ($n = 18$, *E* and *F*), with $\tau = 0.78 \pm 0.32$ min ($n = 11$). With return to $V_j = 0$ mV, $G_j$ recovers to control values, with $\tau = 2.4 \pm 0.9$ min ($n = 4$, *E*). With application of $V_j$ negative at 5R/N side from $V_j = 0$ (*E*) or $V_j = 40$ mV (5R/N side positive, *F*), $G_j$ drops to 35.2 ± 17.3% ($n = 10$) of control values (measured at $V_j = 0$), with $\tau = 1.05 \pm 0.61$ min ($n = 9$). In homotypic 32–32 junctions (*G*), application of 40-mV $V_j$ gradients to either oocyte decreases $G_j$ to 67.7 ± 8.2% ($n = 7$). $G_j$ drops rapidly at first (*G*; more obvious with 1st $V_j$ exposure) and then more slowly; this suggests that $V_j$ affects conventional (fast) and slow $V_j$-sensitive gates. Tandem-32 channels (*H*) and other mutant-32 channels, as well as 32–32 and 5R/N-5R/N channels, are insensitive to $V_m$.

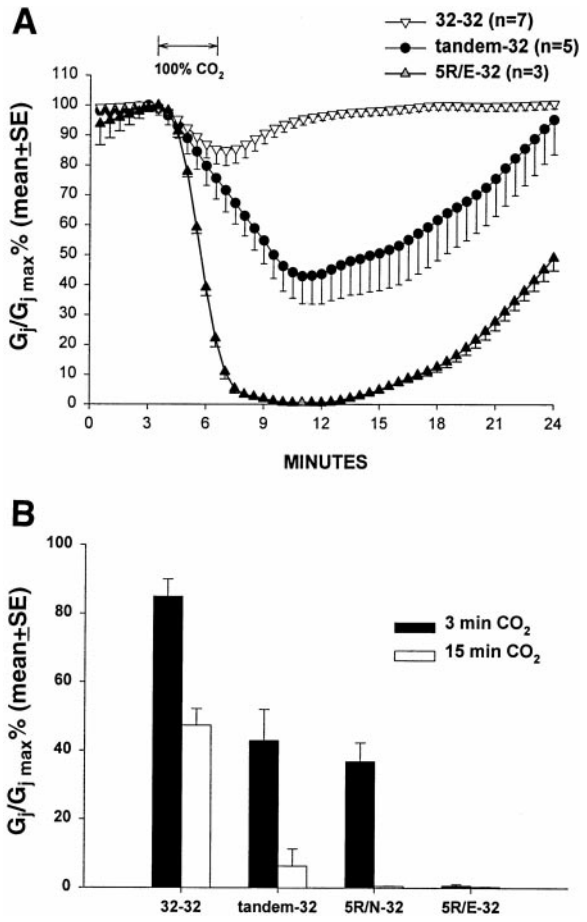


Fig. 4. $G_j$ sensitivity to 100% $CO_2$ of 32–32, tandem-32, and 5R/E-32 channels. With 32–32 channels, $G_j$ decreases to 85 ± 5% (mean ± SE, $n = 7$, *A*) with 3-min exposure to $CO_2$ and to 47 ± 4.8% ($n = 16$, *B*) with 15-min $CO_2$ exposure at a maximum rate of ~9%/min. All heterotypic channels are more $CO_2$ sensitive than 32–32 channels (*B*). With tandem-32 channels, $G_j$ drops to 43 ± 8% ($n = 5$) with 3-min exposures to $CO_2$ (*A* and *B*) and to 6.4 ± 5% ($n = 4$) with 15-min exposures (*B*) at a maximum rate of ~13%/min. 5R/E-32 channels (*A* and *B*) are the most sensitive channels tested in any of our oocyte studies; $G_j$ drops to zero ($n = 3$) with 3-min exposures to $CO_2$ (*A* and *B*) at a maximum rate of ~37%/min (*A*). 5R/N-32 channels are slightly more sensitive than tandem-32 channels; $G_j$ decreases to 37.5 ± 6.4% ($n = 3$) with 3-min exposure to $CO_2$ (*B*) and to ~0% ($n = 4$) with 15-min exposures (*B*) at a maximum rate of ~21%/min. Thus $CO_2$ sensitivity of these channels ranks as follows: 5R/E-32 > 5R/N-32 > tandem-32 > 32–32.

the same. Interestingly, the effect of voltage on chemical gating has been recently reported in insect cells (29). In this case, however, the chemical gate appears to be sensitive to $V_m$ rather than to $V_j$. The idea that the slow gate and the $CO_2$-sensitive gate are the same may be corroborated by the observation that with mutant-32 channels a $V_j$ application (mutant side positive) during $CO_2$-induced uncoupling increases $G_j$ by a much larger fraction than in the absence of $CO_2$. We believe that positive $V_j$ has a greater effect on $G_j$ in the presence than in the absence of $CO_2$, because with $CO_2$ a larger fraction of slow gates are in the closed state. This further indicates that $V_j$ and $CO_2$ compete for driving the same gating mechanism. An additional piece of evidence favoring the idea that the chemical gate and the slow gate may be the same comes from preliminary data on oocytes in which calmodulin (CaM) expression was inhibited with antisense oligonucleotides to CaM mRNA (15, 17). Within 24–48 h after the injection of CaM antisense oligonucleotides, the slow gating behavior of tandem-32, 5R/E-32, and other mutant-32 channels completely disappeared (17) and tandem-32 channels manifested a symmetrical $V_j$ sensitivity virtually identical to that of 32–32 channels. This observation, in conjunction with our previous data showing complete loss of $CO_2$ gating sensitivity after the same treatment with CaM antisense oligonucleotides (15), suggests that CaM may be involved in chemical gating and slow gating mechanisms. On this basis, a gating mechanism viewing CaM (or another small acidic protein) as a negatively charged channel-plugging molecule ("cork" gating model) is being considered (see below).

Data from this and previous studies (25, 27, 28) show that homotypic 5R/N-5R/N and heterotypic tandem-32, 5R/E-32, and 5R/N-32 channels are more sensitive to $CO_2$ than 32–32 channels. If we assume that the hemichannels of heterotypic channels gate independently from each other (27), this would indicate that, in tandem-32, 5R/E-32, and 5R/N-32 pairs, most of the channels close at the mutant hemichannel side. If this were the case, the observed increase in $G_j$ at positive $V_j$ would be expected to reflect primarily the behavior of the slow gates of tandem, 5R/E, and 5R/N hemichannels rather than that of Cx32 hemichannels. Because $V_j$ gradients activate the conventional $V_j$ gate as well, the increase in $G_j$ observed at positive $V_j$ on the mutant side indicates that the consequence of slow gates reopening significantly outweighs the effect of $V_j$ gates closing. Thus the increase in $G_j$ in the presence and absence of $CO_2$ with positive $V_j$ at the mutant side would be even greater if the conventional $V_j$ gate were inactive, and the opposite would be expected with negative $V_j$. However, the effect of 40-mV $V_j$ gradients on conventional $V_j$ gating is relatively small.

With 32–32 channels, $V_j$ gradients of either polarity always caused further drops in $G_j$ during exposure to $CO_2$. Because in this case the $CO_2$-sensitive gates are expected to close symmetrically, one would predict $V_j$ gradients to complement the effect of $CO_2$ at the negative side and oppose it at the positive side; thus the $G_j$ drop may result from the activation of conventional $V_j$-sensitive gates only. However, the magnitude of the $G_j$ drop is greater than expected on the basis of the weak sensitivity of 32–32 channels to $V_j$ gradients of ±40 mV. Therefore, it is likely that the $G_j$ drop reflects the effect of $V_j$ on conventional $V_j$ gates and slow gates.

If it is assumed that the observed phenomena reflect the behavior of a slow gate, why do they manifest themselves preferentially in these mutants? One can only speculate at this stage. In previous studies we have proposed that CL is relevant for $CO_2$-induced gating of Cx32 channels (23, 24) and that $CT_1$ may inhibit gating by limiting CL mobility via electrostatic and hydrophobic interactions with $CL_1$ (26). If present, these interactions could maintain the channel open by latching $CT_1$ to $CL_1$. $CO_2$ would close the channel by

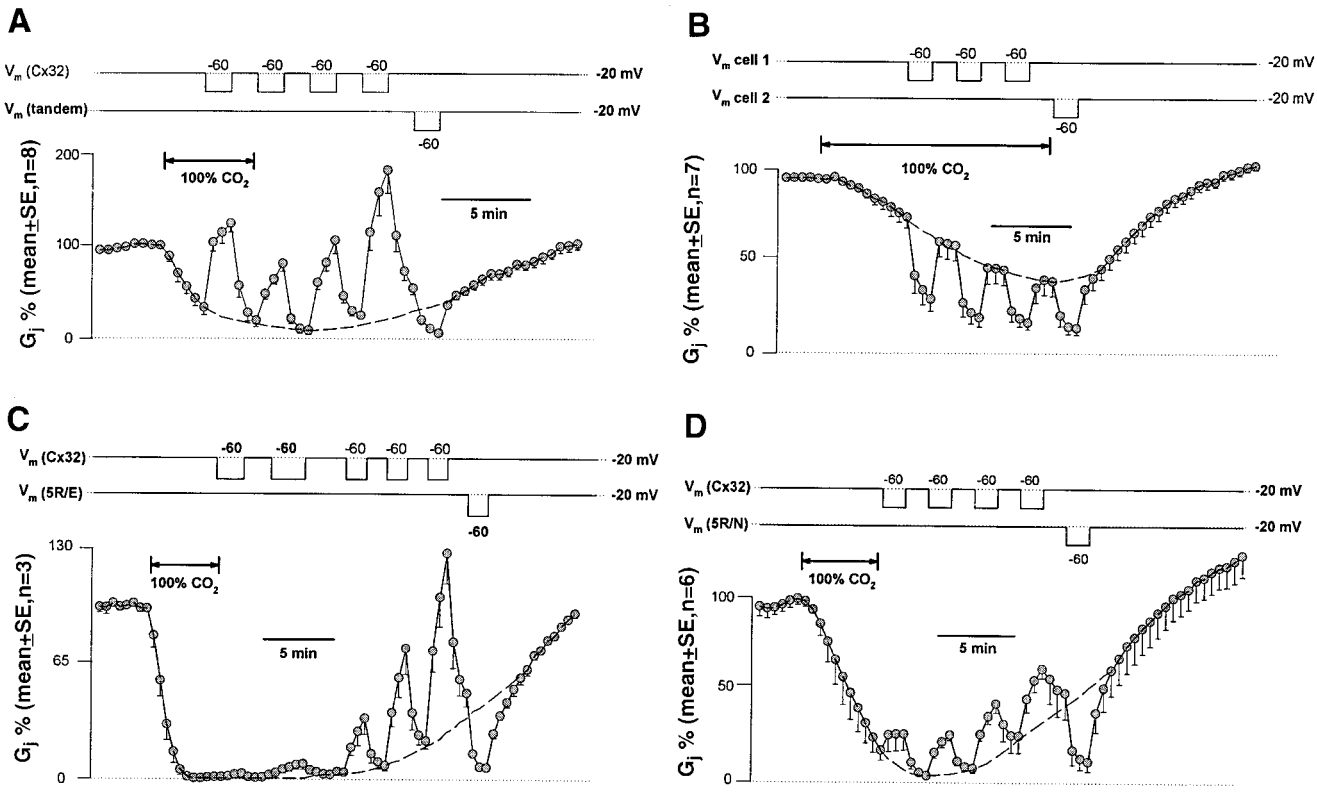


Fig. 5. Effect of $V_j$ on $G_j$ during exposure to 100% $CO_2$ in oocyte pairs expressing tandem-32 (*A*), 32–32 (*B*), 5R/E-32 (*C*), or 5R/N-32 (*D*) channels. $G_j$, reduced to low values by $CO_2$ at $V_j = 0$, increases significantly and reversibly with the application of $V_j$ gradients positive at mutant side (*A*, *C*, and *D*). With similar $V_j$ gradients, $G_j$ increases less at maximal uncoupling. This is more notable with 5R/E-32 channels (*C*); $CO_2$ sensitivity of these channels is so high that $G_j$ remains virtually zero for several minutes (*C*). $V_j$ increases $G_j$ by ~1,000% (*A*, 3rd $V_j$ application), ~2,600% (*C*, 2nd $V_j$ application), and ~600% (*D*, 2nd $V_j$ application) in tandem-32, 5R/E-32, and 5R/N-32 channels, respectively. This is noteworthy, because in absence of $CO_2$, similar $V_j$ applications increase $G_j$ by only ~260, ~180, and ~23%, respectively (Fig. 3, *A* and *C–F*). This indicates that $V_j$ opens mutant-32 channels that had been closed by $CO_2$. $V_j$ negative at mutant side dramatically and reversibly reduces $G_j$ to very low values (*A*, *C*, and *D*). In contrast, with 32–32 channels, $V_j$ gradients of either polarity significantly decrease $G_j$ (*B*). Magnitude of $G_j$ drop (*B*) indicates that also in the case of 32–32 channels $V_j$ affects conventional $V_j$ gate and slow $V_j$ gate. Dashed lines, predicted $G_j$ time course in absence of $V_j$ gradients.

initiating a mechanism that releases CL from CT. If this were true, one would expect any weakening of the $CL_1$-$CT_1$ interaction to result in a mixture of open and closed channels. In tandem, 5R/E, and 5R/N mutants, $CL_1$-$CT_1$ interactions might be weaker for the following reasons. In the tandem mutants, three of the six CT and NT chains are linked, which may prevent three of the six $CT_1$ domains from reaching $CL_1$ domains, if indeed both monomers are inserted in the membrane. In 5R/E mutants the replacement of five basic residues of $CT_1$ (R215, R219, R220, R223, and R224) with acidic residues (E) would cause $CT_1$ and $CL_1$ to repel each other, inasmuch as electrostatic $CL_1$-$CT_1$ interactions are postulated to occur between basic $CT_1$ residues (particularly R215 and R219) (25, 28) and acidic $CL_1$ residues (El02, E109, and D113). In 5R/N mutants the removal of positive charges from $CT_1$ would eliminate electrostatic interactions yet leave unaffected hydrophobic interactions. This would be expected to weaken but not prevent $CT_1$-$CL_1$ interactions, which could be the reason why 5R/N-32 channels were not affected by steady-state $V_j$ gradients as strongly as tandem-32 or 5R/E-32 channels. Consistent with this idea may also be recent data for increased $CO_2$ sensitivity in mutants in which E102 was replaced with R (26) or G (19) residues, mutations that would be expected to weaken potential $CL_1$-$CT_1$ charge interactions; interestingly, the latter is a mutation reported to occur in some patients with Charcot-Marie-Tooth disease (7, 19).

Of course, the $CT_1$-$CL_1$ association-dissociation hypothesis is based on many assumptions, the foremost of which is the $CL_1$-$CT_1$ interaction, which at this stage relies primarily on circumstantial evidence (26). Therefore, the phenomena described here could very well be related to different molecular domains. Whatever conformational changes connexins undergo with uncouplers, a likely possibility is that these changes render the channel mouth more accessible to a negatively charged plugging molecule (cork gating model).

The cork gating hypothesis envisions slightly different scenarios for 32–32 and mutant-32 channels. In the former, CaM would have limited accessibility to the channel mouth under normal cytosolic conditions (absence of uncouplers) and in the absence of $V_j$ gradients. Uncouplers would change CaM and/or connexin conformation, making the channel mouth accessible to a CaM

lobe, which would bind electrostatically and hydrophobically to the channel's mouth, closing the channel completely. The latter would be accessible to a CaM lobe even without uncouplers, but CaM would bind loosely, only electrostatically, such that positive $V_j$ would dislodge it slowly and negative $V_j$ would lodge it in a greater number of channels. With uncouplers, CaM would plug the channel more efficiently, by interacting electrostatically and hydrophobically. This would imply two closed states: *closed state 1* would involve both types of interaction and would not be reversed by $V_j$, and *closed state 2* would involve only electrostatic interactions, and so it would be sensitive to $V_j$. The presence of both types of interaction in *closed state 1* could explain why at maximum uncoupling positive $V_j$ is less effective (Fig. 5*C*). Because the channel's mouth (18) and the CaM lobes are ~2.5 nm in diameter, a CaM lobe could fit well in the channel's mouth.

In conclusion, data on chemical and voltage gating characteristics of three Cx32 mutants (tandem, 5R/E, and 5R/N) expressed heterotypically with Cx32 wild type indicate that $V_j$ gradients activate a slow gating mechanism that appears to be distinct from the conventional $V_j$ gating mechanism. The presumed slow gate opens at relatively positive $V_j$ and closes at negative $V_j$, following exponential courses with long time constants. In addition, a positive $V_j$ at the mutant side appears to reopen channels closed by $CO_2$, raising the possibility that the chemical gate and the $V_j$-sensitive slow gate are the same. The slow gate appears to be present in homotypic Cx32 channels as well, but since these channels are all open in the absence of $V_j$, the slow gate of Cx32 wild-type channels manifests itself only with relatively negative $V_j$ gradients. This gate could be a pluglike cytosolic molecule (possibly CaM).

The authors thank Dr. Eric C. Beyer (Washington University) for providing the cDNA clone for the rat liver connexin32, Dr. Basilio A. Kotsias (Instituto Investigaciónes Médicas, Buenos Aires, Argentina) for useful criticism, and Drs. Peter G. Shrager and Ted B. Begenisich (University of Rochester) for helpful comments on the manuscript.

This study was supported by National Institute of General Medical Sciences Grant GM-20113.

A preliminary account of this study has been published in abstract form (16).

Address for reprint requests and other correspondence: C. Peracchia, Dept. of Pharmacology and Physiology, School of Medicine and Dentistry, University of Rochester, 601 Elmwood Ave., Rochester, NY 14642-8711 (E-mail: cpera@pharmacol.rochester.edu).

Received 6 November 1998; accepted in final form 15 March 1999.

## REFERENCES

1. **Barrio, L. C., T. Suchyna, T. Bargiello, L. X. Xu, R. S. Roginski, M. V. L. Bennett, and B. J. Nicholson.** Gap junctions formed by connexins 26 and 32 alone and in combination are differently affected by applied voltage. *Proc. Natl. Acad. Sci. USA* 88: 8410–8414, 1991.
2. **Bergoffen, J., S. S. Scherer, S. Wang, M. O. Scott, L. J. Bone, D. L. Paul, K. Chen, M. W. Lensch, P. F. Chance, and K. H. Fischbeck.** Connexin mutations in X-linked Charcot-Marie-Tooth disease. *Science* 262: 2039–2042, 1993.
3. **Bruzzone, R., T. W. White, and D. L. Paul.** Connections with connexins: the molecular basis of direct intercellular signaling. *Eur. J. Biochem*. 238: 1–27, 1996.
4. **Bukauskas, F. F., C. Elfgang, K. Willecke, and R. Weingart.** Heterotypic gap junction channels (connexin26-connexin32) violate the paradigm of unitary conductance. *Pflügers Arch*. 429: 870–872, 1995.
5. **Bukauskas, F. F., and C. Peracchia.** Two distinct gating mechanisms in gap junction channels: $CO_2$-sensitive and voltage-sensitive. *Biophys. J*. 72: 2137–2142, 1997.
6. **Ek-Vitorin, J. F., G. Calero, G. E. Morley, W. Coombs, S. M. Tafet, and M. Delmar.** pH regulation of connexin43: molecular analysis of the gating particle. *Biophys. J*. 71: 1273–1284, 1996.
7. **Ionasescu, V., C. Searby, and R. Ionasescu.** Point mutations of the connexin32 (GJB1) gene in X-linked dominant Charcot-Marie-Tooth neuropathy. *Hum. Mol. Genet*. 3: 355–358, 1994.
8. **Liu, S., S. Taffet, L. Stoner, M. Delmar, M. L. Vallano, and J. Jalife.** A structural basis for the unequal sensitivity of the major cardiac and liver gap junctions to intracellular acidification: the carboxyl tail length. *Biophys. J*. 64: 1422–1433, 1993.
9. **Loewenstein, W. R.** Cell-to-cell communication and the control of growth. *Am. Rev. Respir. Dis*. 142: S48–S53, 1990.
10. **Morley, G. E., S. M. Taffet, and M. Delmar.** Intramolecular interactions mediate pH regulation of connexin43 channels. *Biophys. J*. 70: 1294–1302, 1996.
11. **Obaid, A. L., S. J. Socolar, and B. Rose.** Cell-to-cell channels with two independently regulated gates in series: analysis of junctional conductance modulation by membrane potential, calcium, and pH. *J. Membr. Biol*. 73: 69–89, 1983.
12. **Paul, D. L.** Molecular cloning of cDNA for rat liver gap junction protein. *J. Cell Biol*. 103: 123–134, 1986.
13. **Peracchia, C., A. Lazrak, L. L. Peracchia.** Molecular models of channel interaction and gating in gap junctions. In: *Handbook of Membrane Channels. Molecular and Cellular Physiology*, edited by C. Peracchia. San Diego: Academic, 1994, p. 361–377.
14. **Peracchia, C., and X. G. Wang.** Connexin domains relevant to the chemical gating of gap junction channels. *Braz. J. Med. Biol. Res*. 30: 577–590 1997.
15. **Peracchia, C., X. Wang, L. Li, and L. L. Peracchia.** Inhibition of calmodulin expression prevents low-pH-induced gap junction uncoupling in *Xenopus* oocytes. *Pflügers Arch*. 431: 379–387, 1996.
16. **Peracchia, C., X. G. Wang, and L. L. Peracchia.** Is the chemical gate of gap junctions voltage sensitive? (Abstract). *Mol. Biol. Cell* 9: 323A, 1998.
17. **Peracchia, C., X. G. Wang, and L. L. Peracchia.** Connexin32 mutants reveal a slow gate that opens at positive potentials (Abstract). *Biophys. J*. 76: A221, 1999.
18. **Perkins, G., D. Goodenough, and G. Sosinsky.** Three-dimensional structure of the gap junction connexon. *Biophys. J*. 72: 533–544, 1997.
19. **Ressot, C., D. Gomès, A. Dautigny, D. Pham-Dinh, and R. Bruzzone.** Connexin32 mutations associated with X-linked Charcot-Marie-Tooth disease show two distinct behaviors: loss of function and altered gating properties. *J. Neurosci*. 18: 4063–4075, 1998.
20. **Sambrook, J., E. Fritsch, and T. Maniatis.** *Molecular Cloning*. Cold Spring Harbor, NY: Cold Spring Harbor Laboratory Press, 1989.
21. **Spray, D. C., A. L. Harris, and M. V. L. Bennett.** Equilibrium properties of a voltage-dependent junctional conductance. *J. Gen. Physiol*. 77: 77–93, 1981.
22. **Verselis, V. K., C. S. Ginter, and T. A. Bargiello.** Opposite voltage gating polarities of two closely related connexins. *Nature* 368: 348–351, 1994.
23. **Wang, X. G., L. Q. Li, L. L. Peracchia, and C. Peracchia.** Chimeric evidence for a role of the connexin cytoplasmic loop in gap junction channel gating. *Pflügers Arch*. 431: 844–852, 1996.
24. **Wang, X. G., and C. Peracchia.** Connexin32/38 chimeras suggest a role for the second half of the inner loop in gap junction gating by low pH. *Am. J. Physiol*. 271 (*Cell Physiol*. 40): C1743–C1749, 1996.
25. **Wang, X. G., and C. Peracchia.** Positive charges of the initial C-terminus domain of Cx32 inhibit gap junction gating sensitivity to $CO_2$. *Biophys. J*. 73: 798–806, 1997.
26. **Wang, X. G., and C. Peracchia.** Domains of connexin32 relevant to $CO_2$-induced channel gating. In: *Gap Junctions*, edited by R. Werner. Amsterdam, The Netherlands: IOS, 1998, p. 35–39.

27. **Wang, X. G., and C. Peracchia.** Behavior of heteromeric and heterotypic channels in gap junction chemical gating. *J. Membr. Biol.* 162: 169–176, 1998.

28. **Wang, X. G., and C. Peracchia.** Molecular dissection of a basic COOH-terminal domain of Cx32 that inhibits gap junction gating sensitivity. *Am. J. Physiol.* 275 (*Cell Physiol.* 44): C1384–C1390, 1998.

29. **Weingart, R., and F. F. Bukauskas.** Long-chain *n*-alkanols and arachidonic acid interfere with the $V_m$-sensitive gating mechanism of gap junction channels. *Pflügers Arch.* 435: 310–319, 1998.

30. **Werner, R., E. Levine, C. Rabadan-Diehl, and G. Dahl.** Gating properties of connexin32 cell-cell channels and their mutants expressed in *Xenopus* oocytes. *Proc. R. Soc. Lond.* 243: 5–11, 1991.